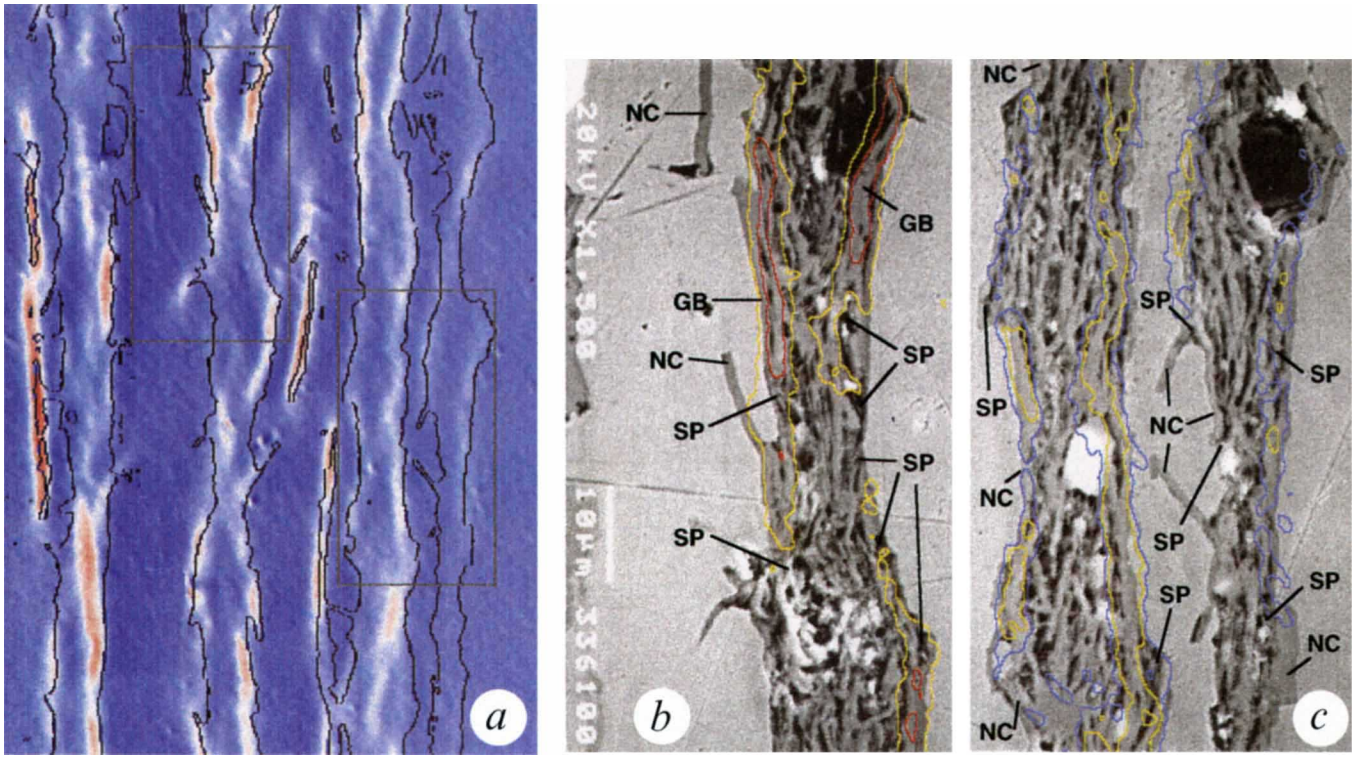

FIG. 3 *a*, Map of the current flow in the superconducting filaments. White and red represent high current density. This pattern is obtained by taking the *x*-derivative of the field maps. Current flow is restricted to narrow regions mostly along the edges of the filaments. A comparison with Fig. 1*a* identifies these regions as phase-pure well aligned Bi-2223. The apparent current flow in isolated regions (marked 'T' in Fig. 1*a*) or outside the superconductor (between the second and third filaments) is caused by the next stack of filaments just under the exposed surface as discussed above. *b* and *c*, microstructure of the areas indicated by boxes in *a*. Overlaid are contour lines of the current density at levels of 1.4×10^5 (red), 0.8×10^5 (yellow) and 0.4×10^5 A cm^{-2} (blue). Second-phase particles (marked 'SP') cause frequent interruptions of the current path, whereas small-angle grain boundaries ('GB') do not degrade current flow. Well textured Bi-2223 grain colonies that carry only little current or no current at all are marked as 'NC'. Scale bar, 10 μm.

or no current at all. These sections are either isolated outgrowths, or are disconnected from a continuous current path due to the positioning of second-phase particles. Small-angle grain boundaries between Bi-2223 grain colonies (misalignment angle $\theta \approx 15°$, see positions marked 'GB' in Figs 1*a* and 3*b*) do not affect the current flow significantly. Current flow from one edge of a filament to the other occurs along misaligned Bi-2223 grain colonies (for example, position marked 'MC' in Fig. 1*a*).

Profiles of the current density at 30 K and 77 K are shown in Fig. 2*b*. The large values at the interfaces are clearly seen. Even at 77 K values of $\sim 8 \times 10^4$ A cm^{-2} are observed. The numerical uncertainties caused by the unknown aspect ratios of the current-carrying grain colonies are <25%. The above expression for the transport current in terms of the field gradient is not valid for the space between the current-carrying grain colonies; thus the negative values for J_c in Fig. 2*b* should be ignored.

In the present sample four interconnections between filaments (marked 'IN' in Fig. 1*a*) are observed, only one of which is found to contribute to current transport. The coupling between filaments is an important parameter for minimizing losses in composite conductors carrying alternating current[14]. Clearly, magneto-optical imaging of transport currents is the ideal way to investigate filament coupling in composites with large filament numbers where interconnections are frequent. □

Received 20 March; accepted 13 June 1995.

1. Larbalestier, D. C. *et al. Physica* C**221,** 299–303 (1994).
2. Grasso, G., Hensel, B., Jeremie, A. & Flükiger, R. *Physica* C**241,** 45–52 (1995).
3. Lelovic, M., Krishnaraj, P., Erot, N. G. & Balachandran, U. *Physica* C**242,** 246–250 (1995).
4. Liu, H. K., Wang, R. K. & Dou, S. X. *Physica* C**229,** 39–46 (1994).
5. Merchant, N., Luo, J. S., Maroni, V. A., Riley, G. N. Jr & Carter, W. L. *Appl. Phys. Lett.* **65,** 1039–1041 (1994).
6. Dorosinskii, L. A. *et al. Physica* C**203,** 149–156 (1992).
7. Vlasko-Vlasov, V. K., Indenbom, M. V. & Polanskii, A. A. in *The Real Structure of High-T_c Superconductors* (ed. Shekhtman, V. Sh.) 111 (Springer, Berlin, 1993).
8. Welp, U. *et al. Physica* C**235–240,** 241–244 (1994).
9. Pashitski, A. E., Polyanskii, A. A., Gurevich, A., Parrell, J. A. & Larbalestier, D. C. *Physica* C**246,** 133–144 (1995).
10. Welp, U. *et al. Appl. Phys. Lett.* **66,** 1270–1272 (1995).
11. Sandhage, K., Carter, W. L. & Riley, G. N. Jr *J. Metals* **43,** 21–25 (1991).
12. Balachandran, U. *et al. J. Metals* **46,** 23–25 (1994).
13. Binns, K. J. & Lawrenson, P. J. *Analysis and Computation of Electric and Magnetic Field Problems* (Pergamon, Oxford, 1963).
14. Wilson, M. N. *Superconducting Magnets* 159–197 (Clarendon, Oxford, 1983).

ACKNOWLEDGEMENTS. This work was supported by the US Department of Energy, Basic Energy Sciences, as part of a DOE programme to develop electric power technology (U.W., G.W.C., W.Z. and U.B.), and the US NSF-Office of Science and Technology Centers (D.O.G.).

Scaling behaviour in the dynamics of an economic index

Rosario N. Mantegna & H. Eugene Stanley

Center for Polymer Studies and Department of Physics, Boston University, Boston, Massachusetts 02215, USA

THE large-scale dynamical properties of some physical systems depend on the dynamical evolution of a large number of nonlinearly coupled subsystems. Examples include systems that exhibit self-organized criticality[1] and turbulence[2,3]. Such systems tend to exhibit spatial and temporal scaling behaviour—power-law behaviour of a particular observable. Scaling is found in a wide range of systems, from geophysical[4] to biological[5]. Here we explore the possibility that scaling phenomena occur in economic systems—especially when the economic system is one subject to precise rules,

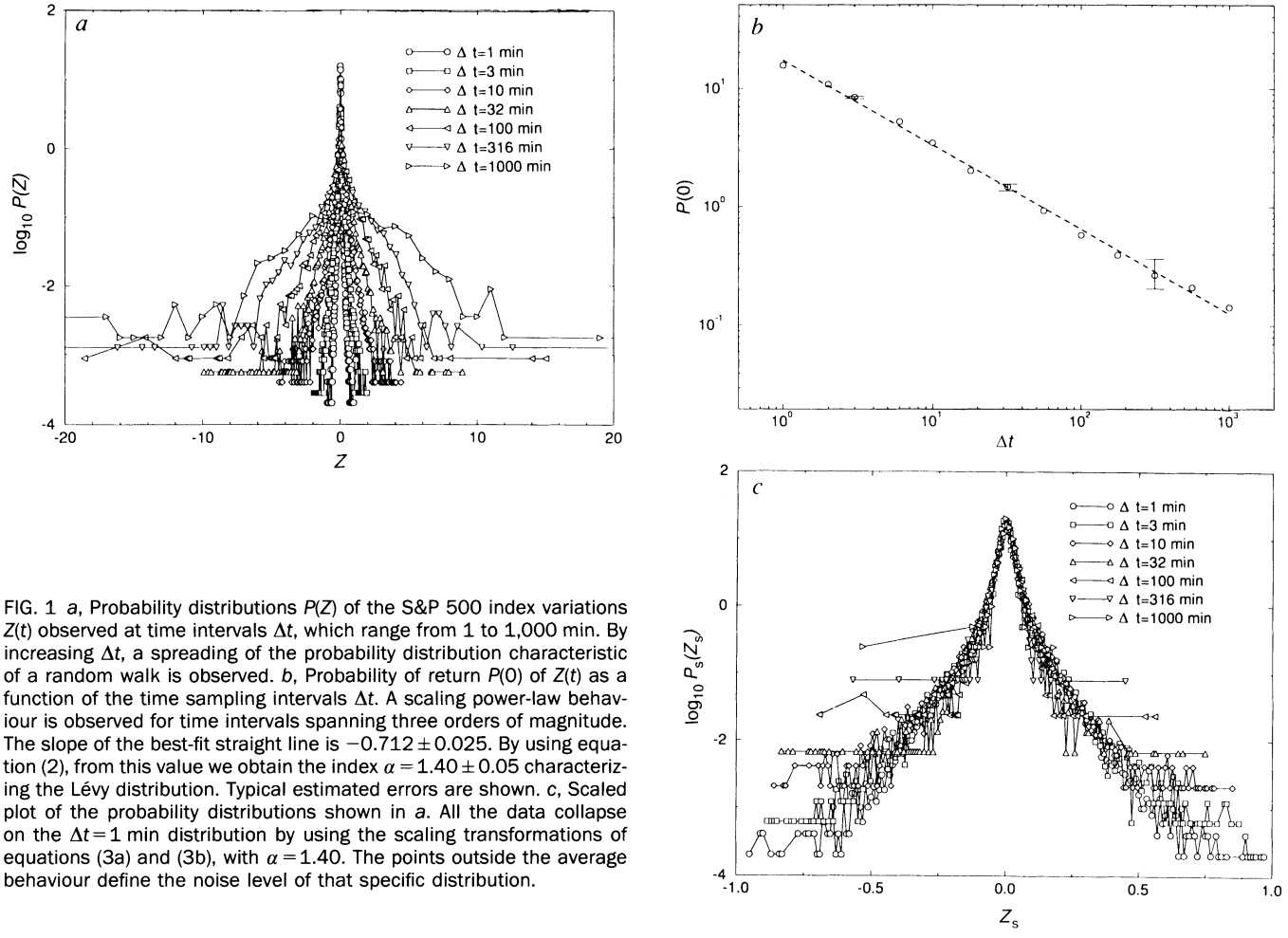

FIG. 1 *a*, Probability distributions $P(Z)$ of the S&P 500 index variations $Z(t)$ observed at time intervals Δt, which range from 1 to 1,000 min. By increasing Δt, a spreading of the probability distribution characteristic of a random walk is observed. *b*, Probability of return $P(0)$ of $Z(t)$ as a function of the time sampling intervals Δt. A scaling power-law behaviour is observed for time intervals spanning three orders of magnitude. The slope of the best-fit straight line is -0.712 ± 0.025. By using equation (2), from this value we obtain the index $\alpha = 1.40 \pm 0.05$ characterizing the Lévy distribution. Typical estimated errors are shown. c, Scaled plot of the probability distributions shown in *a*. All the data collapse on the $\Delta t = 1$ min distribution by using the scaling transformations of equations (3a) and (3b), with $\alpha = 1.40$. The points outside the average behaviour define the noise level of that specific distribution.

as is the case in financial markets[6–8]. Specifically, we show that the scaling of the probability distribution of a particular economic index—the Standard & Poor's 500—can be described by a non-gaussian process with dynamics that, for the central part of the distribution, correspond to that predicted for a Lévy stable process[9–11]. Scaling behaviour is observed for time intervals spanning three orders of magnitude, from 1,000 min to 1 min, the latter being close to the minimum time necessary to perform a trading transaction in a financial market. In the tails of the distribution the fall-off deviates from that for a Lévy stable process and is approximately exponential, ensuring that (as one would expect for a price difference distribution) the variance of the distribution is finite. The scaling exponent is remarkably constant over the six-year period (1984–89) of our data. This dynamical behaviour of the economic index should provide a framework within which to develop economic models.

A problem of interest for both practical and theoretical reasons concerns the distribution of the variations of share price and the dynamical evolution of this distribution. The most widely accepted models state that the variation of share price is a random process. For the distribution of the index returns (which are the difference between two successive logarithms of price), principal proposals include: (1) a normal distribution[12,13], (2) a Lévy stable distribution[14,15], and (3) leptokurtic distributions generated by a mixture of distributions[16], or (4) by ARCH/GARCH models[17,18]. The most obvious difference between the different models involves the wings of the distribution. Distinguishing between the processes by comparing the distribution wings can be quite difficult because data sets are limited. Indeed, different conclusions about the distribution of price variations have been published[12–15,19–24]. In our analysis, we investigate both price difference and returns, and we find the two stochastic processes have quite similar statistical properties in the high-frequency regime.

We have undertaken a statistical study of timescales as short as 1 min, a value close to the minimum time needed to perform a transaction in the market. Specifically, we investigate the dynamics of a price index of one of the largest financial markets in the world: the New York Stock Exchange. We study the Standard & Poor's 500 index during the six-year period from January 1984 to December 1989, and we find that the S&P 500 is a stochastic process remarkably well described by a Lévy stable symmetrical process[25] except for the most rare events. For a time interval spanning three orders of magnitude, the dynamics of the central part of the distribution are in agreement with the predictions of a Lévy stable process.

Data were obtained from the Chicago Mercantile Exchange. They consist of *all* 1,447,514 records of the S&P 500 cash index during the period studied. The time intervals between successive records are not fixed: the average value between successive records is close to 1 min during 1984 and 1985 and close to 15 s during 1986–89. We define the trading time as a continuous time starting from the opening of the day until the closing, and then continuing with the opening of the next trading day. We checked that overnight price differences[26] do not affect the scaling properties of the stochastic process. From this data base, we select the complete set of non-overlapping records separated by a time interval $\Delta t \pm \varepsilon \Delta t$ (where ε is the tolerance, always less than 0.035). We denote the value of the S&P 500 as $y(t)$, and the successive variations of the S&P index is $Z(t) \equiv y(t) - y(t - \Delta t)$.

To characterize quantitatively the experimentally observed process, we first determine the probability distribution $P(Z)$ of index variations for different values of Δt. We select Δt values that are logarithmically equally spaced ranging from 1 to

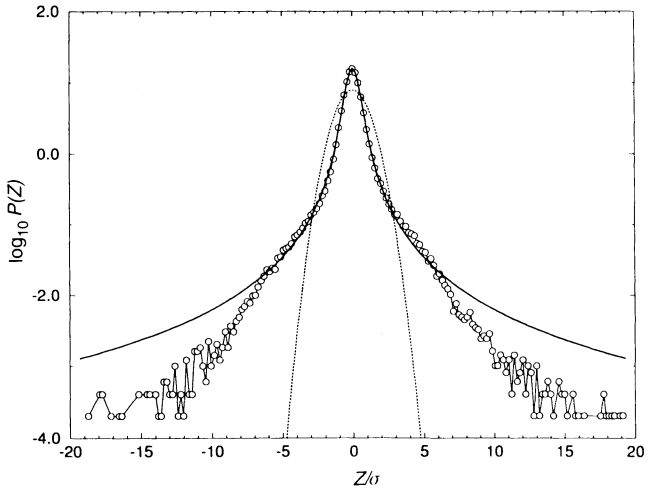

FIG. 2 Comparison of the $\Delta t = 1$ min probability distribution with the symmetrical Lévy stable distribution of index $\alpha = 1.40$ and scale factor $\gamma = 0.00375$ (solid line). The scale factor γ is obtained from equation (2) by using the experimental values of α and $P(0)$. The dotted line shows the gaussian distribution with standard deviation σ equal to the experimental value 0.0508. The variations of price are normalized to this value. Approximately exponential deviations from the Lévy stable profile are observed for $|Z|/\sigma \gtrsim 6$.

1,000 min. The number of data in each set decreases from the maximum value of 493,545 ($\Delta t = 1$ min) to the minimum value of 562 ($\Delta t = 1{,}000$ min).

Figure 1*a* is a semilogarithmic plot of $P(Z)$ obtained for seven different values of Δt. As expected for a random process, the distributions are roughly symmetrical and are spreading when Δt increases. We also note that the distributions are leptokurtic, that is, they have wings larger than expected for a normal process. A determination of the parameters characterizing the distributions is difficult if one uses methods that mainly investigate the wings of distributions, especially because larger values of Δt imply a reduced number of data.

Therefore we use a different approach: we study the 'probability of return' $P(Z=0)$ as a function of Δt. With this choice we investigate the point of each probability distribution that is least affected by the noise introduced by the finiteness of the experimental data set. In Fig. 1*b*, we show $P(0)$ versus Δt in a log–log plot. The data are fitted well by a straight line of slope -0.712 ± 0.025. We observe a non-normal scaling behaviour (slope $\neq -0.5$) in an interval of trading time ranging from 1 to 1,000 min. This experimental finding agrees with the theoretical model of a Lévy walk or Lévy flight[9–11]. In fact, if the central region of the distribution is well described by a Lévy stable symmetrical distribution,

$$L_\alpha(Z, \Delta t) \equiv \frac{1}{\pi} \int_0^\infty \exp(-\gamma \Delta t q^\alpha) \cos(qZ) dq \qquad (1)$$

of index α and scale factor γ at $\Delta t = 1$, where $\exp(-\gamma \Delta t |q|^\alpha)$ is the characteristic function of the symmetrical stable process, then the probability of return is given by

$$P(0) \equiv L_\alpha(0, \Delta t) = \frac{\Gamma(1/\alpha)}{\pi \alpha (\gamma \Delta t)^{1/\alpha}} \qquad (2)$$

where Γ is the Gamma function. By using the value -0.712 ± 0.025 from the data of Fig. 1*b* we obtain the index $\alpha = 1.40 \pm 0.05$.

We also check if the scaling extends over the entire probability distribution as well as $Z = 0$. To this end, we first note that Lévy stable symmetrical distributions rescale under the transformations

$$Z_s \equiv \frac{Z}{(\Delta t)^{1/\alpha}} \qquad (3a)$$

and

$$L_\alpha(Z_s, 1) \equiv \frac{L_\alpha(Z, \Delta t)}{(\Delta t)^{-1/\alpha}} \qquad (3b)$$

Figure 1*c* shows the distributions of Fig. 1*a* plotted in scaled variables. All the data collapse on the $\Delta t = 1$ min distribution when we use equations (3a) and (3b) with $\alpha = 1.40$. From Fig. 1*c* we conclude that a Lévy distribution describes well the dynamics of the probability distribution $P(Z)$ of the random process over time intervals spanning three orders of magnitude.

In Fig. 2, we compare the probability distribution observed for $\Delta t = 1$ min with the Lévy stable distribution of index $\alpha = 1.40$. Note that the solid line is not simply a 'fit' to the data; rather, the appropriate scale factor $\gamma = 0.00375$ is obtained by using the experimental value of $P(0)$ and equation (2). A good agreement with the Lévy (non-gaussian) profile is observed for almost three orders of magnitude when $|Z|/\sigma \lesssim 6$ and an approximately exponential fall-off from the stable distribution is observed for $|Z|/\sigma \gtrsim 6$; here $\sigma = 0.0508$ is the standard deviation. Our results show a clear deviation of the tails of the distribution from the Lévy profile.

The Lévy distribution has an infinite second moment (if $\alpha < 2$). But our experimental finding of an exponential (or stretched exponential) fall-off implies that the second moment is finite, thereby resolving the question of how one could get around the problem of an infinite variance if the Lévy distribution is used to describe the price difference distribution[24]. This conclusion might at first sight seem to contradict our observation of Lévy scaling of the central part of the price difference distribution over fully three orders of magnitude. However, there is no contradiction, because (for example), a recent study[27] finds that Lévy scaling may hold over a long period of time for the dynamics of 'quasi-stable' stochastic processes having a finite variance.

By using the Berry–Esseen theorem[28,29], we can estimate that the maximal time needed to observe convergence for the price differences to a gaussian process is of the order of 1 month. This estimate is obtained by using the experimental values of $\langle |Z|^3 \rangle$ and $\langle Z^2 \rangle$ observed in the high-frequency regime (for example at $\Delta t = 1$ minute). For our data set, we measure $\langle |Z|^3 \rangle = 0.605 \times 10^{-3}$ and $\langle Z^2 \rangle = 0.00257$, and we set an upper bound of the difference between the integral of the distribution and the corresponding asymptotic normal process of 0.1. Our estimate of roughly 1 month is in agreement with an independent empirical study of the distribution of daily, weekly and monthly returns, for which a progressive convergence to a gaussian process is found[30].

We also investigate the scaling properties of $P(0)$ within each year to determine if the scale index α is highly fluctuating from year to year. The results of this analysis are shown in Fig. 3. We also show the line best fitting $P(0)$ of the entire set of data. In different years, the graph of $P(0)$ is always parallel to the overall behaviour (dotted line) in a log–log plot. This implies that the index α is roughly constant over the years. The scale factor γ (related to the vertical position of data in Fig. 3) varies somewhat from year to year. It is higher (lower positions of the experimental points in the figure) for periods of higher 'volatility' (an economic term indicating higher values of the variance of the price variations). When the same analysis is performed monthly, similar conclusions are obtained: α is roughly constant ($\alpha =$

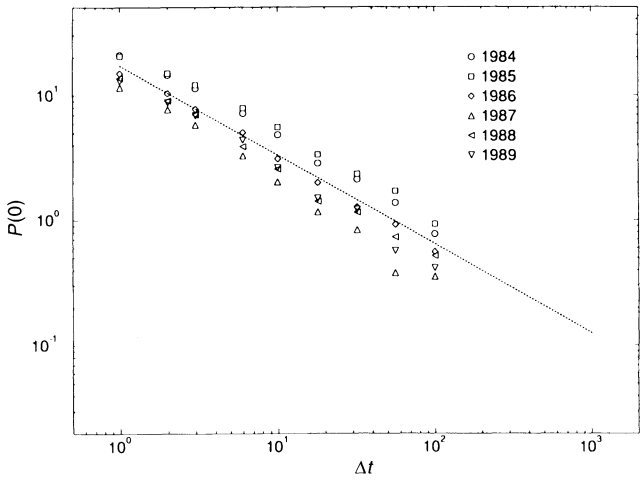

FIG. 3 Probability of return $P(0)$ of the S&P 500 index variations as a function of the time sampling intervals observed in different years. The same scaling behaviour of the complete set of data (dotted line) is observed each year (data are parallel to the dotted line). The scale factor γ is slowly time-dependent, as the vertical positions of the probability of return change from year to year.

1.38 ± 0.14) and γ fluctuates more than α, having bursts of activity localized in specific months (such as April 1987, and October 1987 and immediately following months).

We compare our experimental results with the statistical properties of the heteroskedastic stochastic process GARCH(1, 1) (ref. 18). We simulate GARCH(1, 1) processes characterized by control parameters close to the values obtained in the time-series analysis of stock returns[22]. We find that the time evolution of the probability density functions (PDFs) of the GARCH(1, 1) process is quite different from that observed in the experimental data. In particular, we investigate the probability of return to the origin of the GARCH(1, 1) simulated process using the values of the control parameters selected to mimic the experimental $\Delta t =$ 1 min PDF, and find the data are fitted well by a straight line in a log–log plot, with slope -0.531 ± 0.025. The scaling index is therefore 1.88 ± 0.09, a value close to 2 but 43% larger than the value of 1.4 observed in the experimental data. □

Received 12 September 1994; accepted 1 June 1995.

1. Bak, B., Tang, C. & Wiesenfeld, K. *Phys. Rev. Lett.* **59,** 381–384 (1987).
2. Nelkin, M. *Adv. Phys.* **43,** 143–181 (1994).
3. Meneveau, C. & Sreenivasan, K. R. *J. Fluid. Mech.* **224,** 429–484 (1991).
4. Olami, Z., Feder, H. J. S. & Christensen, K. *Phys. Rev. Lett.* **68,** 1244–1247 (1992).
5. Peng, C.-K. *et al. Phys. Rev. Lett.* **70,** 1343–1346 (1993).
6. Brock, W. A. in *The Economy as a Complex Evolving System* (ed. Anderson, P. W., Arrow, J. K. & Pines, D.) 77–97 (Addison-Wesley, Redwood City, 1988).
7. Brock, W. A., Hsieh, D. A. & LeBaron, B. *Nonlinear Dynamics, Chaos, and Instability: Statistical Theory and Economic Inference* (MIT Press, Cambridge, MA, 1991).
8. Scheinkman, J. A. & LeBaron, B. *J. Business* **62,** 311–327 (1989).
9. Shlesinger, M. F., Frisch, U. & Zaslavsky, G. (eds) *Lévy Flights and Related Phenomena in Physics* (Springer, Berlin, 1995).
10. Bouchaud, J.-P. & Georges, A. *Phys. Rep.* **195,** 127–293 (1990).
11. Shlesinger, M. F., Zaslavsky, G. M. & Klafter, J. *Nature* **363,** 31–37 (1993).
12. Bachelier, L. J. B. *Théorie de la Speculation* (Gauthier-Villars, Paris, 1900).
13. Osborne, M. F. M. *Oper. Res.* **7,** 145–173 (1959).
14. Mandelbrot, B. B. *J. Business* **36,** 394–419 (1963).
15. Fama, E. F. *J. Business* **38,** 34–105 (1965).
16. Clark, P. K. *Econometrica* **41,** 135–155 (1973).
17. Engle, R. F. *Econometrica* **50,** 987–1007 (1982).
18. Bollerslev, T., Chou, R. Y. & Kroner, K. F. *J. Econometrics* **52,** 5–59 (1992).
19. Officer, R. R. *J. Am. statist. Ass.* **67,** 807–812 (1972).
20. Hsu, D.-A., Miller, R. B. & Wichern, D. W. *J. Am. statist. Ass.* **69,** 108–113 (1974).
21. Lau, A. H.-L., Lau, H.-S. & Wingender, J. R. *J. Business Econ. Statist.* **8,** 217–223 (1990).
22. Akgiray, V. *J. Business* **62,** 55–80 (1989).
23. Mantegna, R. N. *Physica* **A179,** 232–242 (1991).
24. Tucker, A. L. *J. Business Econ. Statist.* **10,** 73–81 (1992).
25. Lévy, P. *Théorie de l'Addition des Variables Aléatoires* (Gauthier-Villars, Paris, 1937).
26. Brock, W. A. & Kleidon, A. W. *J. Econ. Dyn. Contr.* **16,** 451–489 (1990).
27. Mantegna, R. N. & Stanley, H. E. *Phys. Rev. Lett.* **73,** 2946–2949 (1994).
28. Shlesinger, M. F. *Phys. Rev. Lett.* **74,** 4959 (1995).
29. Feller, W. *An Introduction to Probability Theory and Its Applications* (Wiley, New York, 1971).
30. Akgiray, V. & Booth, G. G. *J. Business Econ. Statist.* **6,** 51–57 (1988).

ACKNOWLEDGEMENTS. We thank S. V. Buldyrev and K. Simons for important contributions in the early stages of this work, and J. Gonzalo, M. A. Salinger and S. Zapperi for helpful discussions. This work was supported by the US NSF.

Dynamics of formation of symmetrical patterns by chemotactic bacteria

Elena O. Budrene* & Howard C. Berg*†

* Department of Molecular and Cellular Biology, Harvard University, 16 Divinity Avenue, Cambridge, Massachusetts 02138, USA
† Rowland Institute for Science, 100 Edwin H. Land Boulevard, Cambridge, Massachusetts 02142, USA

MOTILE cells of *Escherichia coli* aggregate to form stable patterns of remarkable regularity when grown from a single point on certain substrates. Central to this self-organization is chemotaxis, the motion of bacteria along gradients of a chemical attractant that the cells themselves excrete[1]. Here we show how these complex patterns develop. The long-range spatial order arises from interactions between two multicellular aggregate structures: a 'swarm ring' that expands radially, and focal aggregates that have lower mobility. Patterning occurs through alternating domination by these two sources of excreted attractant (which we identify here as aspartate). The pattern geometries vary in a systematic way, depending on how long an aggregate remains active; this depends, in turn, on the initial concentration of substrate (here, succinate).

Under certain conditions, cells of chemotactic strains of *Escherichia coli* and *Salmonella typhimurium* excrete an attractant, aggregate in response to gradients of that attractant, and form patterns of varying cell density[1–3]. This process occurs only if cells are chemotactic towards aspartate, and can be suppressed by addition of aspartate or aspartate analogues. In *E. coli*, aggregates form in the wake of a travelling circular band, producing highly symmetrical patterns[1]. Their geometry depends on initial conditions; for example, the concentration of growth substrate. In *S. typhimurium*, aggregates arise from the centre of an unstructured bacterial lawn, producing patterns with lower symmetry[2]. The present work was undertaken to determine the mechanism by which *E. coli* forms patterns with long-range spatial order and why particular geometries arise at different initial concentrations of substrate. Succinate and fumarate both work well[1]; we used succinate.

Patterns appear within a certain range of succinate concentrations (Fig. 1). The concentrations of growth substrate required for each pattern vary from strain to strain, but for a given strain, the succession of patterns observed with increasing concentrations is fixed. At low concentrations of succinate, one sees a single compact travelling band (swarm ring) that moves slowly outwards (Fig. 1*a*). At higher concentrations, spots appear in concentric rings in radial rows (that is, on a pseudo-rectangular lattice), Fig. 1*b*, then in sets of intersecting spirals (that is, on a pseudo-hexagonal lattice), Fig. 1*c*, and finally on a pseudo-hexagonal lattice but with radial tails, Fig. 1*d*. As evident in Fig. 1*d* and documented below, the spots form in the wake of a band of cells moving outwards at the periphery of the pattern. An unstructured zone of low cell density always precedes the first element of a pattern. The radius of this zone decreases with increasing concentration of substrate. The radial periods and circumferential spacings differ from strain to strain, from about 1 to 6 mm. At even higher concentrations of substrate, one obtains more elaborate patterns, with radial streaks, indented rings, or petals (not shown). These patterns are not as reproducible, even in replicate plates, and some geometries appear only with certain strains.

To understand how changes in one initial condition, the concentration of succinate, can so dramatically alter the pattern-forming behaviour of the system, we studied effects of succinate concentration on bacterial growth and chemotaxis. The growth rate of *E. coli* in succinate saturates and is approximately constant over the concentration range 0.5–7 mM, in agreement with